SUPPLEMENTAL MATERIAL

Supplemental Methods

In Vitro Studies

CPCs and DOXO Treatment. Clonogenic c-kit-positive CPCs obtained by cell sorting and single cell cloning were infected with a retrovirus carrying EGFP and employed in these studies.[1] CPCs were treated for 12, 24 and 48 h with 0.1, 0.5 and 1 μM DOXO concentrations (Adriblastina, Pharmacia&Upjohn). DOXO doses are comparable to peak or steady state plasma concentrations observed in patients after standard bolus infusion.[2]

Cell Viability Assay. MTT (3-(4,5-Dimethylthiazol-2-yl)-2,5-diphenyltetrazolium bromide) assay was used to determine cytotoxicity of DOXO. Yellow MTT is reduced to purple formazan when mitochondrial reductase enzymes are active. This conversion is directly related to the number of living cells. Optical density (OD) was measured at 540 nm with spectrophotometer.

TUNEL Assay. Terminal deoxynucleotidyltransferase (TdT)–mediated dUTP nick end labeling (TUNEL) assay was used for the detection of apoptosis[3,4] with ApoAlert DNA fragmentation kit (Clontech).

DNA Fragmentation. Total DNA was extracted from control and DOXO-treated CPCs using Wizard Genomic Promega DNA Purification Kit. DNA pellets were dissolved in TE buffer (pH 7.4) and equal amounts of DNA were resolved with 1.5% agarose gel[5] and stained with SYBR Green (Molecular Probes).

Caspase-3 Activity. Cells were washed with ice-cold PBS and lysed with cell lysis buffer (ApoAlert Caspase-3 Colorimetric Assay kit, Clontech Laboratories). Samples were incubated on ice and centrifuged at 12,000 g for 10 min at 4°C. Caspase-3 activity in the supernatant was measured in a microplate reader (Bio-Rad), using DEVD-*p*-nitroanilide as a substrate.

CPC Proliferation. One hour before the end of the experiment, CPCs were incubated with BrdU (10 μM). Cell proliferation was determined by the number of BrdU-positive CPCs.[1,4] CPCs in mitosis were identified by phospho-H3 antibody (Upstate).

Western Blotting. Cells were lysed in buffer containing 0.1% Triton X100 and a cocktail of protease inhibitors (Sigma-Aldrich). Protein concentration was measured by Bradford assay (Bio-Rad). Protein extracts were then separated on 8-12% SDS-PAGE and transferred onto PVDF membrane (Amersham). Antibody binding was visualized by ECL (SuperSignal West Femto Maximum Sensitivity Substrate, Pierce Biotechnology) and OD of the bands was analyzed with Molecular Analysis software (Bio-Rad). Loading conditions were determined by the expression of β-actin (Sigma-Aldrich). Primary antibodies against cyclin D1 (Zymed), cdk4, cyclin B1, $p16^{INK4a}$, cdc2, $p21^{Cip}$, $p27^{Kip1}$, Bax (Santa Cruz Biotechnology), phospho-cdc2, Rb, phospho-Rb, p53, phospho-$p53^{Ser15}$, phospho-$p53^{Ser20}$, ATM kinase, Bad (Cell Signaling), Mn-SOD, Cu/Zn-SOD (Upstate) and catalase (Sigma-Aldrich) were used. Peroxidase-conjugated secondary antibodies (Santa Cruz Biotechnology) were employed.

CPCs and Oxidative Stress. Oxidative stress in CPC was determined by immunolabeling with 8-OH-dG mouse monoclonal antibody[4] (QED Bioscience).

Antioxidant Enzyme Activity. Protein extracts from control and DOXO-treated CPCs were prepared by sonication and centrifugation at 2,500 g for 10 min.

SOD Activity. The activity of Cu/Zn-SOD and Mn-SOD was measured by employing a superoxide dismutase kit (R&D). Samples were incubated with a xanthine/xanthine oxidase solution. The generation of superoxide ions converts NBT to NBT-diformazan. SOD present in the sample decreases superoxide ion concentration reducing the rate of NBT-diformazan formation. The extent of reduction in the appearance of NBT-diformazan is a measure of SOD activity present in the cell lysates.[6] The absorbance of non reducted NBT was measured at 560 nm.

Catalase activity. This parameter was measured according to the modified method developed by Cohen.[7] Cell lysates were incubated for 5 min with 6 mM H_2O_2 at room

temperature. The reaction was quenched by the addition of 0.6 N H_2SO_4 and 10 mM $FeSO_4$. The colorimetric reaction of the formed products was obtained by adding potassium thiocyanate (KSCN). The absorbance of the ferrithiocyanate product was measured at 490 nm.

Telomerase Activity and Telomere Length. Telomerase activity[8,9] was measured by quantitative PCR with a commercially available kit (Chemicon). The assay consisted of a one step real time PCR reaction. PCR products were detected by measuring the increase in fluorescence caused by binding of SYBR Green to double-strand DNA, which correspond to telomeric repeats generated by the active telomerase present in CPC lysates. HeLa cells were used as positive control and RNase-treated samples as negative control. Serial dilution of proteins was employed. Telomere length was evaluated in cytospins of CPCs by quantitative fluorescence in situ hybridization (Q-FISH) and confocal microscopy.[4,8,10] A fluorescein isothiocyanate-peptide nucleic acid (FITC-PNA) probe was used. The fluorescent signals measured in lymphoma cells with short (L5178Y-S, 7 kbp) and long (L5178Y-R, 48 kbp) telomeres were utilized to compute absolute telomere length.

Quantitative RT-PCR Array. The transcriptional profile of CPCs in the absence and presence of DOXO was assessed by quantitative RT-PCR array in 5 cases. This quantitative analysis involved a restricted panel of genes with SYBR Green-optimized primer assays (supplementary Figure IV). Arrays containing a panel of stem cell related genes (SuperArray) and custom-designed panels of lineage-related and senescence-associated genes were performed. In each case, 3 x 10^6 CPCs were sent to the SuperArray facility (SABiosciences) for RNA isolation, hybridization and data analysis.

In Vivo Studies

Female Fischer 344 rats (n=160) at 3 months of age (body weight 180±10 g) received 6 i.p. injections of 2.5 mg/kg b.w. of DOXO over a period of 2 weeks to reach a cumulative dose of 15 mg/kg b.w.[11] Control rats were injected with saline. Animals were sacrificed at 3 weeks and 6 weeks after the first injection of DOXO (supplementary Figure III). In a

third group of animals, CPCs were delivered intramyocardially (supplementary Figure V). Under ketamine (100 mg/kg b.w., i.p.) and acepromazine (1 mg/kg b.w., i.p.) anesthesia, rats were intubated, thoracotomy performed and the heart was exposed. A total of 5 x 10^4 EGFP-labeled CPCs were injected at 4 sites in the left ventricular myocardium. CPCs were suspended in PBS together with polystyrene microspheres conjugated with rhodamine (Molecular Probes) for the identification of the sites of injection and confirmation of successful administration of cells.[12,13] Control rats were injected with PBS. BrdU was injected twice a day (50 mg/kg b.w., i.p.) and added to the drinking water (1 mg/ml) to identify newly formed cells.[1,4,8,10,14] Rats were sacrificed 3 weeks after surgery, i.e., 6 weeks after the first injection of DOXO.

Echocardiography and Hemodynamics. Rats were anesthetized with ketamine (100 mg/kg b.w., i.p.), and echocardiographic parameters were collected with a high resolution Micro-Ultrasound system System (Vevo 770, VisualSonics Inc.) equipped with a 25-MHz linear transducer. Body temperature was maintained at ~37°C with a heating pad. Serial M-mode echocardiographic images were taken in the short axis view at the level of the papillary muscles. Left ventricular diameter and posterior wall thickness were measured in diastole and systole and fractional shortening and ejection fraction were calculated.[1,4,10,12] At sacrifice, hemodynamic parameters were collected. Animals were anesthetized with sodium pentobarbital (50 mg/kg body weight, i.p.), and the right carotid artery was cannulated with a microtip pressure transducer (SPR-612, Millar Instruments) connected to an A/D converter (iWorx 214) and a computer system. The catheter was advanced into the LV cavity for the evaluation of LV pressures and + and − dP/dt in the closed-chest preparation.[1,4,10,12,13]

Fixation of the Heart. After the collection of hemodynamic measurements, the abdominal aorta was cannulated with a polyethylene catheter filled with phosphate buffer (0.2 M, pH 7.4) and heparin (100 IU/ml). In rapid succession, the heart was arrested in diastole by injection of cadmium chloride (100 mM) through the aortic catheter, the thorax was opened, perfusion with phosphate-buffered formalin was started, and the right

atrium was cut to allow drainage. Perfusion pressure was adjusted to the mean arterial pressure.[1,4,8,10,12,13] The left ventricular chamber was filled with fixative from a pressure reservoir set at a height equivalent to the in vivo measured LVEDP. This was accomplished by inserting a 25G3/4 Vacutainer (Becton Dickinson) into the LV chamber. After fixation, the heart was dissected and the weights of the right ventricle and LV inclusive of the interventricular septum were obtained. After measuring the major longitudinal axis, the LV was sectioned serially into five rings perpendicular to the longitudinal axis of the heart, and the thickness of the free wall and septum was determined (ImagePro software). Similarly, the transverse diameter of the LV chamber was evaluated. The transverse and longitudinal diameters were employed to compute chamber volume.[15] Tissue specimens were embedded in paraffin and histological sections were obtained for immunohistochemistry.

Myocyte Size and Number. For the evaluation of myocyte volume and number,[4,10,12,13,15] left ventricular tissue sections were stained with α-sarcomeric actin antibody (Sigma-Aldrich) and propidium iodide (PI). Morphometric sampling consisted of counting by confocal microscopy the number of myocyte nuclear profiles in an area of tissue section in which cardiac muscle cells were cut perpendicularly. Inner and outer layers of each LV were analyzed to determine the number of nuclear profiles per unit area of myocardium, N(n)A, and the volume fraction of myocytes, V(m)V. Nuclear length, D(n), was obtained from measurements in longitudinally oriented myocytes. Number of myocytes per unit volume of myocardium, N(m)V was calculated from:

$$N(m)V = N(n)A / D(n).$$

Myocyte cell volume, V(m), was computed from the volume fraction of myocytes in the tissue, V(m)V, and the number of myocytes per unit volume of myocardium, N(m)V:

$$V(m) = V(m)V / N(m)V$$

The total number of myocytes in the LV, N(m)T, was derived from the product of the number of myocytes per unit volume, N(m)V, and the total LV volume, VT. The latter

was evaluated by dividing ventricular weight by the specific gravity of muscle tissue, 1.06 g/cm^3.

$$N(m)T = N(m)V \times VT.$$

CPC Number. CPCs were identified by using a c-kit antibody (R&D). Morphometric measurements consisted of counting by confocal microscopy the number of CPCs per unit area N(cpc)A, of LV myocardium. Additionally, the average diameter of CPCs, D(cpc), was obtained and the number of CPCs per unit volume of myocardium, N(cpc)V, was calculated utilizing the Schwartz-Saltykov equation.[15,16] The number of CPCs that reached replicative senescence and irreversible growth arrest[4,10] was evaluated by the expression of the senescence-associated protein p16^{INK4a}. The fraction of CPCs undergoing apoptosis[3,4,10] was evaluated by TdT labeling.

Immunohistochemistry. Tissue sections, 4 μm in thickness, were employed for immunolabeling and confocal microscopy.[1,3,4,8,10,12,13,16] Myocytes were identified by α-sarcomeric actin (Sigma-Aldrich), endothelial cells by von Willebrand factor (Sigma-Aldrich), smooth muscle cells by α-smooth muscle actin (Sigma-Aldrich) and cell coupling was established by the presence of connexin 43 (Sigma-Aldrich). Oxidative stress in the nuclei was determined by 8-OH-dG mouse monoclonal antibody[4] (QED Bioscience). EGFP (Invitrogen) labeling was used to identify the progeny of CPCs. Cycling cells were identified by Ki-67 (Vector) and BrdU (Roche) labeling. Secondary antibodies from Jackson ImmunoResearch, were employed to detect primary antibodies (supplementary Table I). Cell death was measured by TdT assay (Clontech Laboratories). DAPI (Sigma-Aldrich) was used to identify the nuclei.

PCR for Detection of EGFP DNA. For PCR detection of EGFP, paraffin sections were obtained from the heart of rats in which EGFP-positive structures were previously detected by immunohistochemistry. Tissue sections were deparaffinized and genomic DNA was extracted with the QIAamp DNA kit (Qiagen). DNA, 100 ng, was mixed with primers for EGFP (EGFP-F: 5'-ATGGTGAGCAAGGGCGAGGAGCTG-3' and EGFP-R: 5'-GCCGT-CGTCCTTGAAGAAGATGGTG-3'). Cycling conditions were as follows:

94°C for 30 sec, followed by 30 cycles of amplification (94°C for 30 sec, 62°C for 30 sec, 72°C for 30 sec), with a final incubation at 72°C for 3 min.[4,8,13] PCR products were run onto agarose gel for the detection of the EGFP band (amplicon size: 315 bp). Tail of β-actin-EGFP mice was used as positive control while tissue sections from rats injected with PBS were used as negative controls.

Myocardial Regeneration. The newly formed myocardium within the heart was identified by the detection of EGFP cells in animals injected with CPCs. The detection of EGFP cells was used to recognize not only myocytes but also vascular endothelial cells (ECs) and smooth muscle cells (SMCs) organized in coronary vessels. The volume of the regenerated myocardium was determined by measuring in three sections, obtained from the base to the apex of the heart, the area occupied by the restored tissue and section thickness. The product of these two variables yielded the volume of tissue repair in each section. Values in the three sections were added, and the total volume of formed myocardium was obtained.[15] EGFP-labeled coronary vessels were evaluated quantitatively. Briefly, the axial ratio (major diameter/minor diameter) for each vascular profile was obtained to assess the angle of orientation of the vessels with respect to the plane of sectioning. This approach allowed us to correct for section orientation and underestimation of vascular profiles per unit area of tissue. The sum of the axial ratios of EGFP-positive vessels per unit area of tissue yielded vessel length per unit volume of myocardium.[10,12,13,15]

Myocyte Isolation. Following sodium pentobarbital anesthesia (150 mg/kg body weight, i.p.), the heart was excised and left ventricular (LV) myocytes were enzymatically dissociated.[17,18] Briefly, the myocardium was perfused retrogradely through the aorta at 37°C with a Ca^{2+}-free solution gassed with 85% O_2 and 15% N_2. After 5 minutes, 0.1 mM $CaCl_2$, 274 units/mL collagenase (type 2, Worthington) and 0.57 units/mL protease (type XIV, Sigma, St. Louis, MO) were added to the solution which contained (mM): NaCl 126, KCl 4.4, $MgCl_2$ 5, HEPES 5, Glucose 22, Taurine 20, Creatine 5, Na Pyruvate

5 and NaH_2PO_4 5 (pH 7.4, adjusted with NaOH). At completion of digestion, the LV was cut in small pieces and re-suspended in Ca^{2+} 0.1 mM solution.[17,18]

Myocyte Mechanics and Ca^{2+} Transients. Isolated LV myocytes were placed in a bath on the stage of an Axiovert Zeiss Microscope for contractility and Ca^{2+} transients measurements. Experiments were conducted at room temperature. Cells were bathed continuously with a Tyrode solution containing (mM): NaCl 140, KCl 5.4, $MgCl_2$ 1, HEPES 5, Glucose 5.5 and $CaCl_2$ 1.0 (pH 7.4, adjusted with NaOH). Measurements were performed in field-stimulated cells at 1 Hz by using IonOptix fluorescence and contractility systems. Contractions were elicited by rectangular depolarizing pulses, 3 ms in duration, and twice-diastolic threshold in intensity, by platinum electrodes.[17,18] Changes in mean sarcomere length were computed by determining the mean frequency of sarcomere spacing by fast Fourier transform and then frequency data were converted to length.[17] Ca^{2+} transients were measured by epifluorescence after loading myocytes with 10 μM Fluo-3 AM (Invitrogen). Excitation length was 480 nm with emission collected at 535 nm using a 40x oil objective. Fluo-3 signals were expressed as normalized fluorescence (F/F_0).

Data Analysis and Statistics. Results are presented as mean±SD. The n values and magnitude of sampling for each determination are listed in supplementary Table II. Significance between two comparisons was determined by unpaired and paired Student's *t*-test and among multiple comparisons by Bonferroni test. Mortality was measured by log-rank test.[10,12,13,15] All *P* values are two-sided and $P<0.05$ was considered to be significant.

Supplemental Table I. Antibodies and their Labeling

Antigen	Antibody	Labeling	Fluorochrome(s)
Stem cell marker			
c-kit	goat polyclonal	indirect	F, T
Structural proteins of myocardial cells			
α-sarcomeric actin	mouse monoclonal	indirect	T, Cy5
Tropomyosin	mouse monoclonal	indirect	T, Cy5
α-smooth muscle actin	mouse monoclonal	direct, indirect	T, Cy5,
von Willebrand factor	sheep polyclonal	indirect	Cy5
Adhesion molecules			
connexin 43	rabbit polyclonal	direct, indirect	T, Cy5
N-cadherin	mouse monoclonal	indirect	T, Cy5
Other stainings			
EGFP	rabbit polyclonal	direct, indirect	F, T, Alexa 488
	goat polyclonal	indirect	F, T
Collagen type I	goat polyclonal	indirect	F, Cy5
Collagen type III	goat polyclonal	indirect	F, Cy5
Ki67	rabbit polyclonal	indirect	F, T, Cy5
Phospho-H3	rabbit polyclonal	indirect	T
BrdU	mouse monoclonal	indirect	T
$p16^{INK4a}$	mouse monoclonal	indirect	T
8-OH-dG	mouse monoclonal	indirect	T

Direct labeling: Primary antibody conjugated with the fluorochrome. Indirect labeling: species-specific secondary antibody conjugated with the fluorochrome. F: fluorescein isothiocyanate, T: tetramethyl rhodamine isothiocyanate, Cy5: cyanine 5.

Supplemental Table II. Magnitude of Sampling

Parameter	n	Aggregate	Mean±SD
In vitro studies			
MTT assay			
12 h			
Control	4	N/A	N/A
0.1 μM DOXO	4	N/A	N/A
0.5 μM DOXO	4	N/A	N/A
1 μM DOXO	4	N/A	N/A
24 h			
Control	4	N/A	N/A
0.1 μM DOXO	4	N/A	N/A
0.5 μM DOXO	4	N/A	N/A
1 μM DOXO	4	N/A	N/A
48 h			
Control	4	N/A	N/A
0.1 μM DOXO	4	N/A	N/A
0.5 μM DOXO	4	N/A	N/A
1 μM DOXO	4	N/A	N/A
BrdU Labeling			
12 h			
Control	3	2289[(1)]	763±46
0.1 μM DOXO	4	2849[(1)]	712±220
0.5 μM DOXO	3	2474[(1)]	825±79
1 μM DOXO	4	2337[(1)]	584±195
24 h			
Control	4	2990[(1)]	748±113

0.1 μM DOXO	3	2018[(1)]	673±68
0.5 μM DOXO	3	2052[(1)]	684±119
1 μM DOXO	3	2306[(1)]	769±177
48 h			
Control	3	2484[(1)]	828±162
0.1 μM DOXO	4	2740[(1)]	685±110
0.5 μM DOXO	4	2772[(1)]	693±194
1 μM DOXO	4	3308[(1)]	827±53
Phospho-H3 Labeling			
12 h			
Control	3	2289[(1)]	763±76
0.1 μM DOXO	3	2403[(1)]	801±142
0.5 μM DOXO	3	2073[(1)]	691±161
1 μM DOXO	3	2186[(1)]	729±254
24 h			
Control	3	2361[(1)]	787±121
0.1 μM DOXO	3	1923[(1)]	641±215
0.5 μM DOXO	4	2703[(1)]	676±235
1 μM DOXO	4	2610[(1)]	653±65
48 h			
Control	3	2551[(1)]	850±62
0.1 μM DOXO	3	2128[(1)]	709±111
0.5 μM DOXO	3	2086[(1)]	695±82
1 μM DOXO	4	2458[(1)]	615±87
8-OH-dG Labeling			
12 h			
Control	3	2618[(1)]	873±84
0.1 μM DOXO	3	2638[(1)]	879±112

0.5 μM DOXO	3	1898[(1)]	633±81
1 μM DOXO	3	1921[(1)]	640±314
24 h			
Control	3	1997[(1)]	666±164
0.1 μM DOXO	3	2184[(1)]	728±204
0.5 μM DOXO	3	1977[(1)]	659±221
1 μM DOXO	3	2016[(1)]	672±180
48 h			
Control	3	2481[(1)]	827±82
0.1 μM DOXO	3	1919[(1)]	640±129
0.5 μM DOXO	3	2177[(1)]	726±273
1 μM DOXO	3	1828[(1)]	609±186
Apoptosis Labeling			
12 h			
Control	3	1942[(1)]	647±126
0.1 μM DOXO	4	2906[(1)]	727±175
0.5 μM DOXO	3	2150[(1)]	717±215
1 μM DOXO	3	2302[(1)]	767±160
24 h			
Control	3	2395[(1)]	798±152
0.1 μM DOXO	4	2751[(1)]	688±56
0.5 μM DOXO	3	2174[(1)]	725±174
1 μM DOXO	3	2465[(1)]	822±81
48 h			
Control	3	1993[(1)]	664±200
0.1 μM DOXO	3	1975[(1)]	658±289
0.5 μM DOXO	3	1939[(1)]	646±109
1 μM DOXO	3	1860[(1)]	620±55
Caspase 3 activity			

12 h			
Control	3	N/A	N/A
0.1 μM DOXO	3	N/A	N/A
0.5 μM DOXO	3	N/A	N/A
1 μM DOXO	3	N/A	N/A
24 h			
Control	3	N/A	N/A
0.1 μM DOXO	3	N/A	N/A
0.5 μM DOXO	3	N/A	N/A
1 μM DOXO	3	N/A	N/A
48 h			
Control	3	N/A	N/A
0.1 μM DOXO	3	N/A	N/A
0.5 μM DOXO	3	N/A	N/A
1 μM DOXO	3	N/A	N/A
DNA Laddering			
12 h			
Control	4	N/A	N/A
0.1 μM DOXO	4	N/A	N/A
0.5 μM DOXO	4	N/A	N/A
1 μM DOXO	4	N/A	N/A
24 h			
Control	4	N/A	N/A
0.1 μM DOXO	4	N/A	N/A
0.5 μM DOXO	4	N/A	N/A
1 μM DOXO	4	N/A	N/A
48 h			
Control	4	N/A	N/A
0.1 μM DOXO	4	N/A	N/A

0.5 μM DOXO	4	N/A	N/A
1 μM DOXO	4	N/A	N/A
Western Blotting			
Cu/Zn SOD			
12 h	16	N/A	N/A
24 h	16	N/A	N/A
48 h	16	N/A	N/A
Mn SOD			
12 h	20	N/A	N/A
24 h	20	N/A	N/A
48 h	20	N/A	N/A
Catalase			
12 h	12	N/A	N/A
24 h	12	N/A	N/A
48 h	12	N/A	N/A
$p21^{Cip}$			
12 h	12	N/A	N/A
24 h	12	N/A	N/A
48 h	12	N/A	N/A
$p16^{INK4a}$			
12 h	12	N/A	N/A
24 h	12	N/A	N/A
48 h	12	N/A	N/A
$p27^{Kip1}$			
12 h	12	N/A	N/A
24 h	12	N/A	N/A
48 h	12	N/A	N/A
Cyclin D1			
12 h	12	N/A	N/A
24 h	12	N/A	N/A

48 h	12	N/A	N/A
Cdk4			
12 h	16	N/A	N/A
24 h	16	N/A	N/A
48 h	16	N/A	N/A
Cyclin B1			
12 h	12	N/A	N/A
24 h	12	N/A	N/A
48 h	12	N/A	N/A
Cdc2			
12 h	12	N/A	N/A
24 h	12	N/A	N/A
48 h	12	N/A	N/A
Phospho cdc2			
12 h	12	N/A	N/A
24 h	12	N/A	N/A
48 h	12	N/A	N/A
Rb			
12 h	16	N/A	N/A
24 h	16	N/A	N/A
48 h	16	N/A	N/A
Phospho Rb			
12 h	16	N/A	N/A
24 h	16	N/A	N/A
48 h	16	N/A	N/A
p53			
12 h	20	N/A	N/A
24 h	20	N/A	N/A
48 h	20	N/A	N/A
Phospho p53$^{(Ser15)}$			

12 h	20	N/A	N/A
24 h	20	N/A	N/A
48 h	20	N/A	N/A
Bcl-2			
12 h	12	N/A	N/A
24 h	12	N/A	N/A
48 h	12	N/A	N/A
Bax			
12 h	12	N/A	N/A
24 h	12	N/A	N/A
48 h	12	N/A	N/A
Bad			
12 h	12	N/A	N/A
24 h	12	N/A	N/A
48 h	12	N/A	N/A
Catalase activity			
12 h			
Control	4	N/A	N/A
0.1 μM DOXO	4	N/A	N/A
0.5 μM DOXO	4	N/A	N/A
1 μM DOXO	4	N/A	N/A
24 h			
Control	4	N/A	N/A
0.1 μM DOXO	4	N/A	N/A
0.5 μM DOXO	4	N/A	N/A
1 μM DOXO	4	N/A	N/A
48 h			
Control	4	N/A	N/A
0.1 μM DOXO	4	N/A	N/A
0.5 μM DOXO	4	N/A	N/A

1 μM DOXO	4	N/A	N/A
SOD activity			
12 h			
Control	4	N/A	N/A
0.1 μM DOXO	4	N/A	N/A
0.5 μM DOXO	4	N/A	N/A
1 μM DOXO	4	N/A	N/A
24 h			
Control	4	N/A	N/A
0.1 μM DOXO	4	N/A	N/A
0.5 μM DOXO	4	N/A	N/A
1 μM DOXO	4	N/A	N/A
48 h			
Control	4	N/A	N/A
0.1 μM DOXO	4	N/A	N/A
0.5 μM DOXO	4	N/A	N/A
1 μM DOXO	4	N/A	N/A
Telomerase Activity			
Control	3	N/A	N/A
DOXO	3	N/A	N/A
Telomere Length			
Control	4	102[(2)]	26±22
DOXO	4	416[(2)]	139±47
Gene Arrays			

Control	5	N/A	N/A
DOXO	5	N/A	N/A
In vivo studies			
Myocyte number and volume			
Control	7	1011[(2)]	144±11
DOXO-3wks	8	1375[(2)]	172±35
DOXO-6wks	8	1126[(2)]	141±17
Fraction of $p16^{INK4a}$-Positive myocytes			
Control	8	1832[(2)]	229±88
DOXO-3wks	9	2301[(2)]	256±143
DOXO-6wks	8	1866[(2)]	233±127
Fraction of Apoptotic Myocytes			
Control	7	359808[(2)]	1401±19847
DOXO-3wks	13	330281[(2)]	25406±7957
DOXO-6wks	11	426519[(2)]	38774±20960
Fraction of Cycling Myocytes			
Control	10	339062[(2)]	33906±16598
DOXO-3wks	13	653027[(2)]	50233±17872
DOXO-6wks	11	351323[(2)]	31938±10938
Number of CPCs			
Control	9	1719[(3)]	191±92
DOXO-3wks	14	2491[(3)]	178±157
DOXO-6wks	11	1983[(3)]	180±80
Fraction of $p16^{INK4a}$-Positive CPCs			

Control	7	302[3]	43±14
DOXO-3wks	9	298[3]	33±18
DOXO-6wks	8	425[3]	53±16
Fraction of Apoptotic CPCs			
Control	9	1686[3]	187±123
DOXO-3wks	8	1978[3]	247±73
DOXO-6wks	11	3566[3]	324±154
Fraction of Cycling CPCs			
Control	9	527[3]	59±23
DOXO-3wks	13	2944[3]	226±73
DOXO-6wks	11	3403[3]	309±164
Fraction of 8-OH-dG-Positive CPCs			
Control	6	271[3]	45±21
DOXO-3wks	6	210[3]	35±16
DOXO-6wks	7	376[3]	54±68
PCR for detection of EGFP DNA			
Control	6	N/A	N/A
DOXO-Untreated	6	N/A	N/A
DOXO-CPCs	6	N/A	N/A
Anatomy			
Control	17	N/A	N/A
DOXO-Untreated	10	N/A	N/A
DOXO-CPCs	17	N/A	N/A
Hemodynamics			

Control	8	N/A	N/A
DOXO-Untreated	6	N/A	N/A
DOXO-CPCs	5	N/A	N/A
Echocardiography			
Control	17	N/A	N/A
DOXO-3wks	8	N/A	N/A
DOXO-6wks	5	N/A	N/A
DOXO-Untreated	6	N/A	N/A
DOXO-CPCs	9	N/A	N/A
Myocyte Mechanics			
Control	3	95	32±9
DOXO	3	78	26±8
Mortality			
Control	12	N/A	N/A
DOXO-Untreated	82	N/A	N/A
DOXO-CPCs	24	N/A	N/A

(1) Number of counted cells; (2) Number of nuclei analyzed; (3) Area of tissue sampled, mm^2; N/A, not applicable.

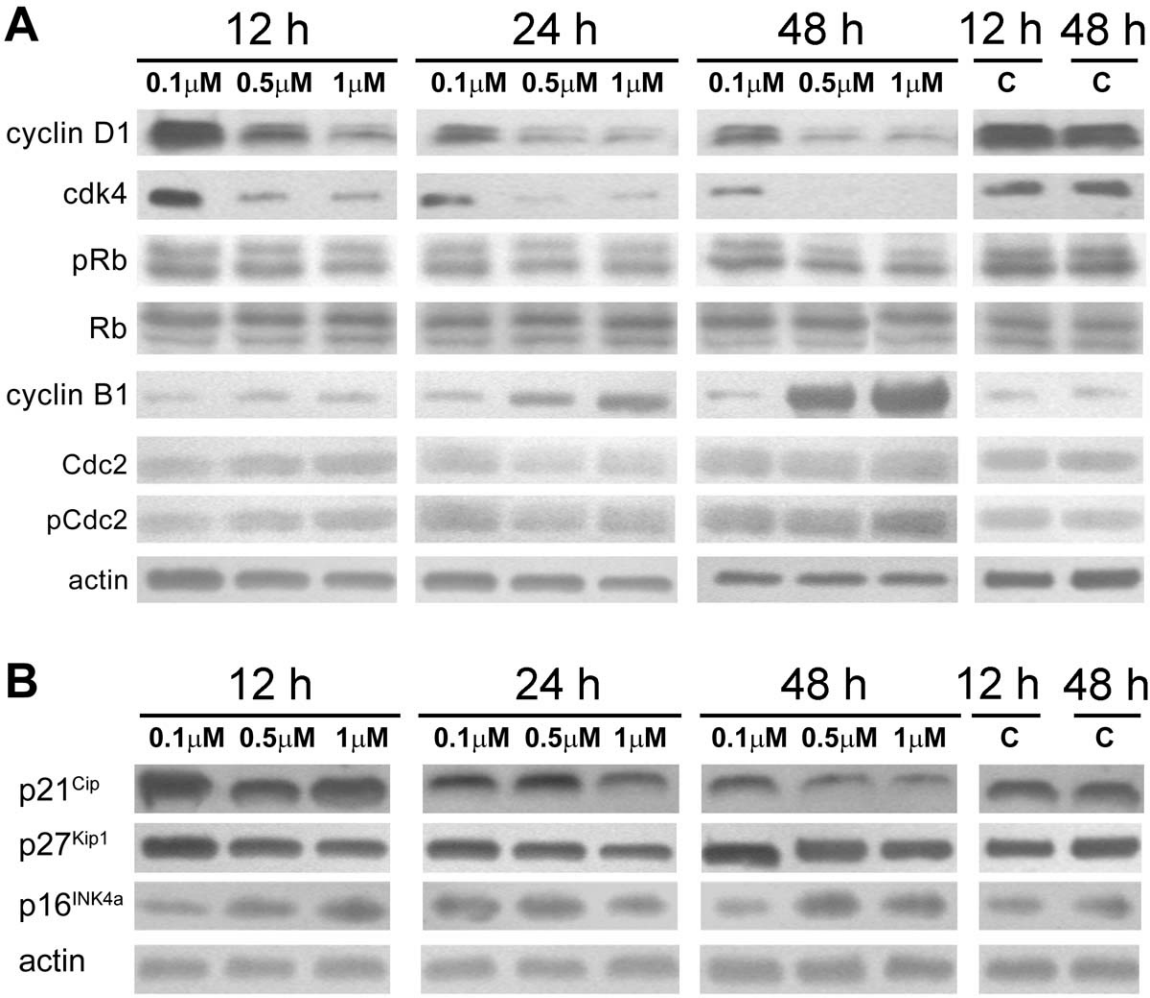

Supplemental Figure I

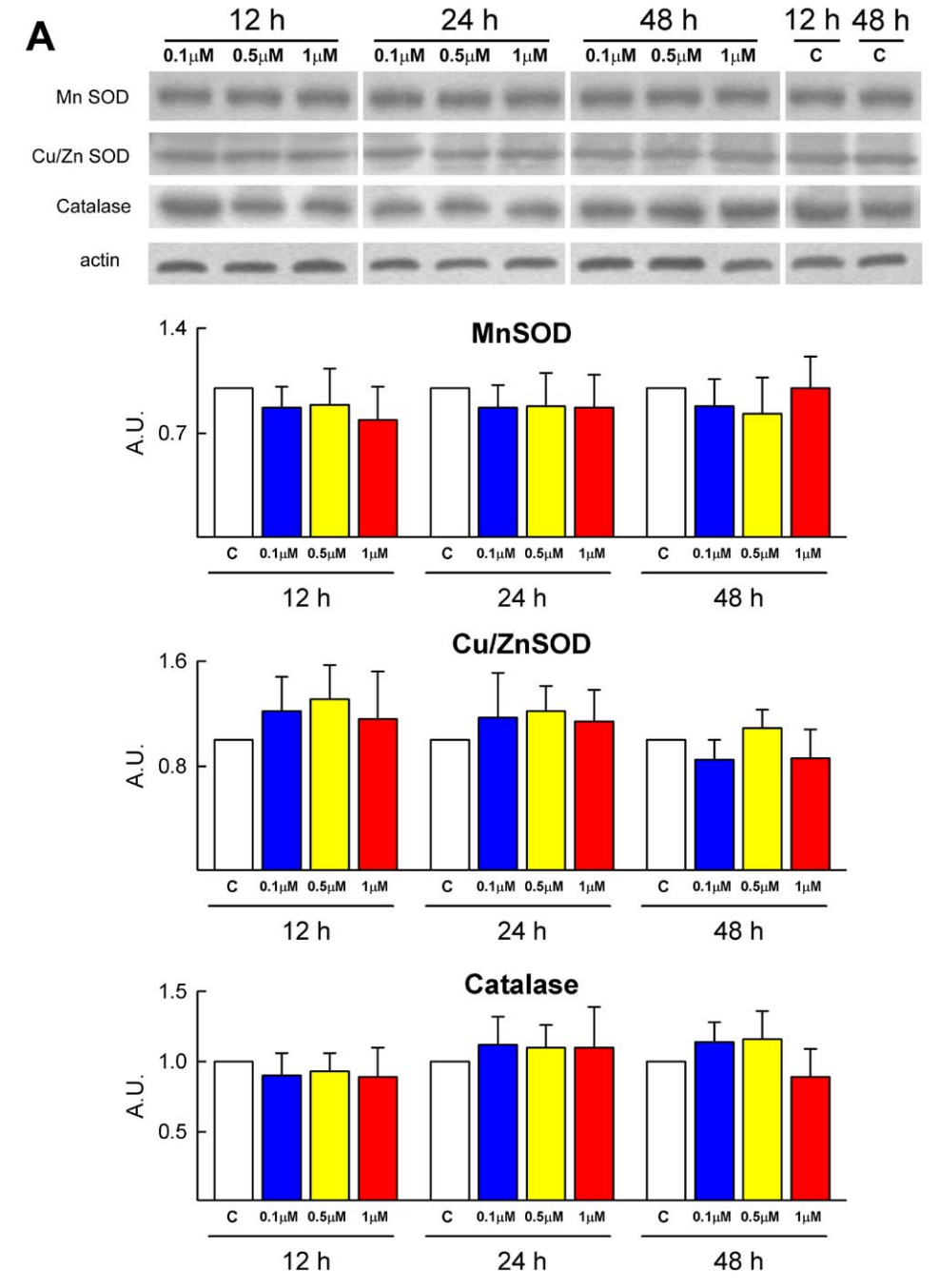

Supplemental Figure II

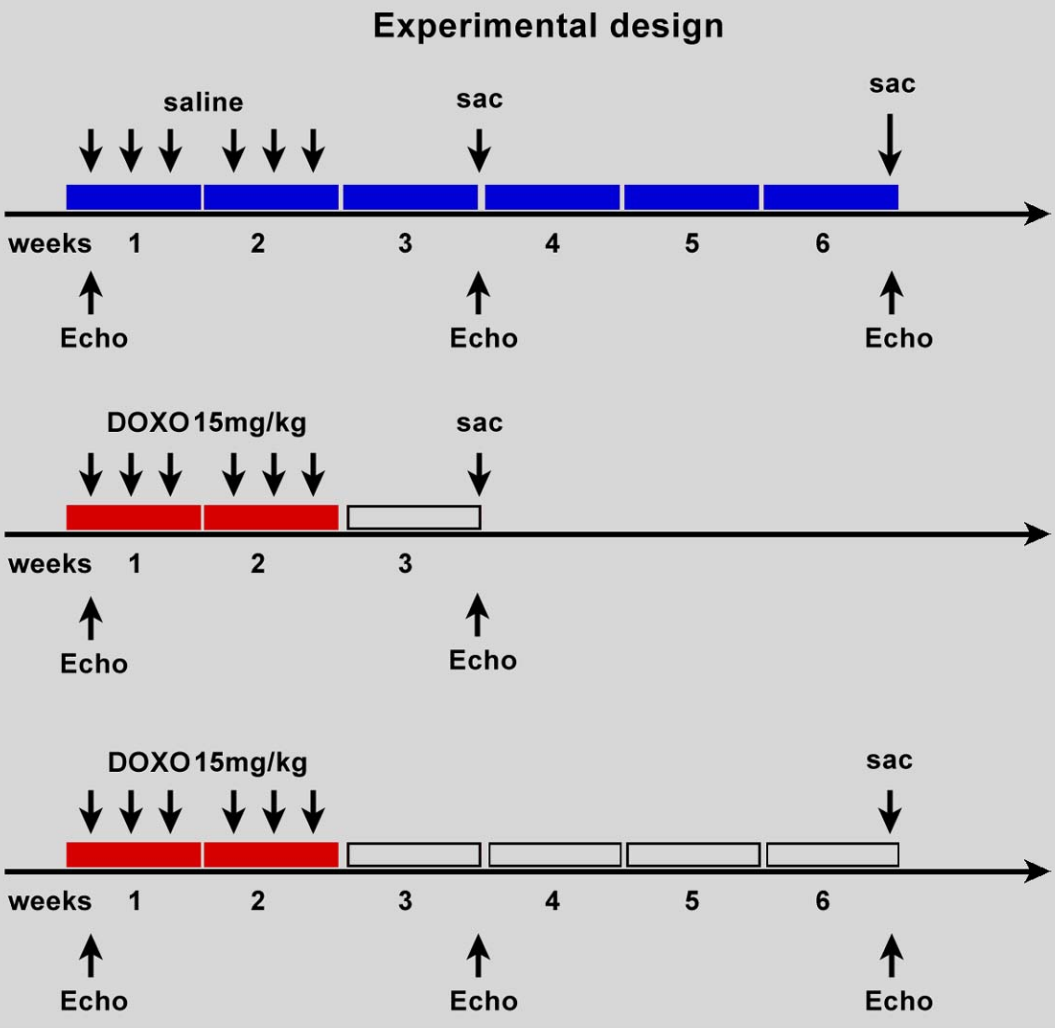

Supplemental Figure III

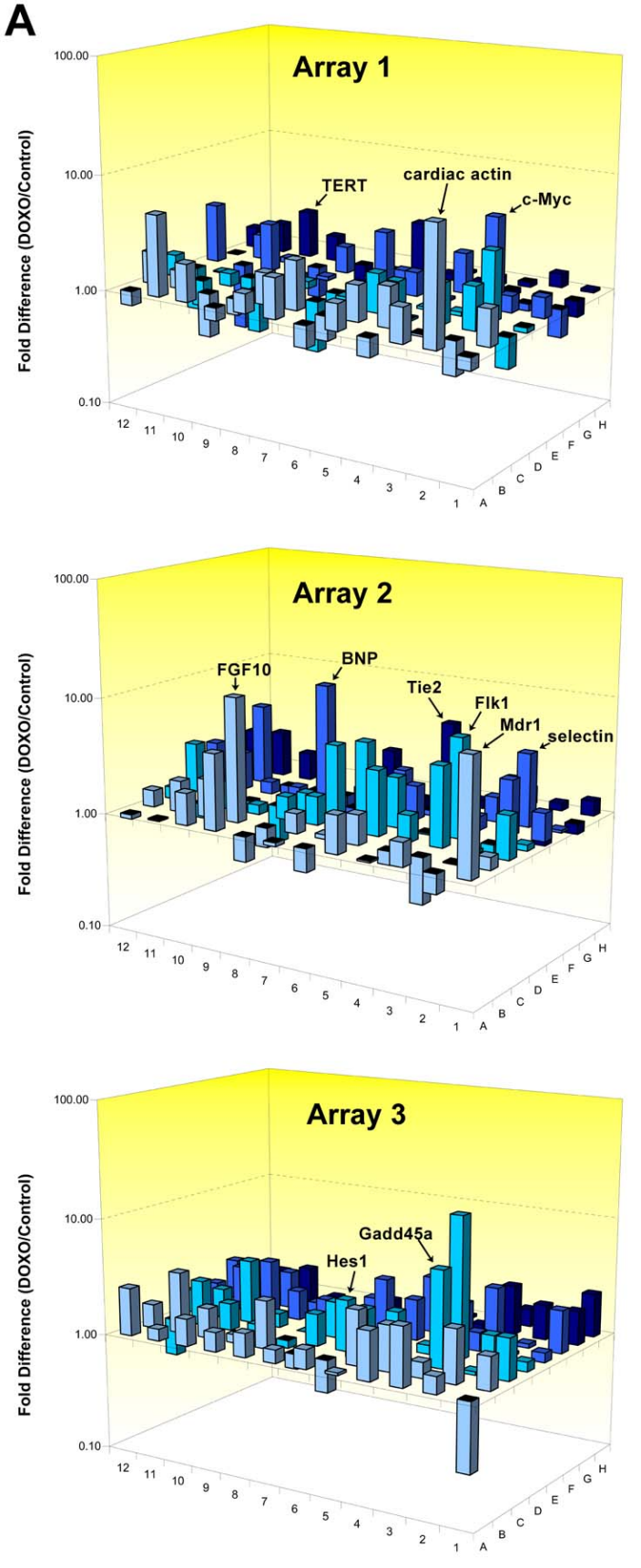

Supplemental Figure IV A

B

Array 1

Gene	Fold	p-value
Abcg2	-1.33	0.3480
Actc1	12.27	0.0001
Adar	1.99	0.0000
Agc1	-1.45	0.0001
Aldh1a1	1.66	0.0045
Aldh2	-1.51	0.0846
Alpi	2.28	0.0098
Apc	1.48	0.0000
Ascl2	-1.47	0.2083
Axin1	2.13	0.0000
Bglap2	5.16	0.0000
Bmp1	-1.33	0.0465
Bmp2	2.05	0.0001
Bmp3	-1.68	0.0948
Btrc	-1.03	0.7928
Ccna2	2.22	0.0000
Ccnd1	2.03	0.0000

Gene	Fold	p-value
Ccnd2	-1.78	0.1379
Ccne1	2.65	0.0000
Cd19	1.98	0.4747
Cd3d	-1.30	0.2720
Cd3e	-2.89	0.0740
Cd4	1.79	0.1647
Cd44	1.89	0.0001
Cd8a	-1.82	0.2260
Cd8b	2.09	0.0200
Cdc2a	2.19	0.0000
Cdc42	-1.05	0.4083
Cdh1	2.52	0.0288
Cdh2	1.22	0.0717
Col1a1	-2.70	0.0000
Col2a1	1.32	0.1994
Col9a1	-3.03	0.0790
Catna1	1.28	0.0002

Gene	Fold	p-value
Cxcl12	-1.68	0.0000
Dhh	1.78	0.1277
Dll1	-1.06	0.6816
Dll3	3.91	0.0002
Dtx2	1.08	0.4375
Dvl1	1.05	0.6952
Ep300	1.55	0.0103
Fgf1	-1.26	0.1178
Fgf2	-1.32	0.2182
Fgf3	1.15	0.0344
Fgf4	1.04	0.6801
Fgfr1	-1.26	0.0084
Foxa2	-1.03	0.9118
Fzd1	-2.35	0.0000
Gcn5l2	1.51	0.0001
Gja1	1.39	0.0000
Gjb1	1.29	0.5954

Gene	Fold	p-value
Hdac1	1.04	0.7288
Hdac2	1.61	0.0001
Hspa9a	3.20	0.0000
Igf1	-1.24	0.3053
Ihh	1.31	0.5657
Isl1	-1.26	0.7534
Jag1	2.60	0.0000
Ka15	-3.72	0.0000
EloA2	4.25	0.0234
Mme	-1.73	0.0000
Msx1	-1.10	0.5493
Myc	5.08	0.0000
Myod1	2.08	0.1065
Myst1	1.94	0.0001
Myst2	1.28	0.0367
Ncam1	-1.05	0.4473
Neurog2	1.57	0.0489

Gene	Fold	p-value
Notch1	-1.92	0.0018
Notch2	1.11	0.0846
Numb	1.62	0.0011
Oprs1	-1.02	0.7433
Pard6a	-1.36	0.0143
Pdx1	1.05	0.9299
Ppard	-1.10	0.3245
Pparg	1.06	0.6749
Rb1	1.12	0.2881
Gdf3	1.82	0.3452
Sox2	-1.21	0.7280
S100b	-1.37	0.0034
T	1.79	0.1864
Tert	2.70	0.0050
Tubb3	1.84	0.0010
Wnt1	1.46	0.3068

Array 2

Gene	Fold	p-value
Abcb1b	9.23	0.0000
Ace	-1.47	0.0040
Acta1	1.69	0.0432
Angpt4	-1.05	0.6640
Atp1a2	2.10	0.0004
Atxn1	-1.60	0.0003
Cald1	-1.09	0.4235
Cd14	-1.66	0.0020
Cd34	4.21	0.0042
Cdh5	1.74	0.0409
Cerberus	-1.12	0.7599
Cryptic	-1.10	0.8972
Cfl2	1.23	0.3507
Calponin2	-1.03	0.7652
Col3a1	-2.50	0.0000
Col4a2	-1.31	0.0150
Crebbp	1.76	0.0005

Gene	Fold	p-value
Dkk1	1.06	0.7123
Dkk4	1.44	0.0528
Epas1	-1.49	0.0023
Fgf10	6.97	0.0114
Fgf8	1.90	0.0423
Flt1	1.83	0.0008
Foxh1	1.28	0.4290
Foxm1	2.28	0.0000
Frzb	1.16	0.7255
Gata1	3.55	0.0120
Gata4	1.65	0.0007
Gata5	3.56	0.0024
Gata6	-1.01	0.9221
Hand1	1.81	0.1031
Hand2	1.58	0.0049
Hdac3	1.19	0.0573
Hdac4	1.71	0.0007

Gene	Fold	p-value
Hdac7a	-1.34	0.0181
Icam2	1.25	0.5594
Igf1r	1.11	0.2091
Kcnj8	-1.33	0.0739
Kdr	6.44	0.0000
Kit	-1.04	0.7131
Klf4	2.65	0.0000
Klf5	4.81	0.0000
Ldb2	3.90	0.0001
Mb	2.22	0.1637
Mef2c	-2.11	0.0006
Mesp1	-1.24	0.4877
Mesp2	1.42	0.1822
Mmrn1	2.61	0.0316
Myh11	1.69	0.0009
Myh7	2.41	0.0916
Myh7b	1.30	0.0384

Gene	Fold	p-value
Myocd	-1.03	0.9385
Myom2	2.05	0.2587
Nkx2-5	1.18	0.0707
eNos	-1.80	0.0012
Nppb	10.78	0.0000
Pdk4	1.24	0.0512
Pecam	1.26	0.0487
Pou5f1	2.47	0.0331
Prox1	2.19	0.0079
Rod1	1.05	0.3330
Sele	5.26	0.0026
Smad4	1.63	0.0000
Smad7	2.48	0.0005
Smtn	-1.11	0.0234
Snai2	2.05	0.0000
Sox5	-1.36	0.0003
Sox6	-1.63	0.0001

Gene	Fold	p-value
Ptk7	-1.35	0.0308
Tagln	-1.25	0.0051
Tal1	5.29	0.0000
Tbx1	3.00	0.0071
Tbx18	-1.22	0.0054
Tbx2	-1.51	0.1428
Tbx20	1.95	0.0019
Tbx5	1.18	0.0707
Tek	5.35	0.0000
Tgfb1	-1.30	0.0785
Tgfbr1	2.40	0.0000
Tnnt2	-1.26	0.0165
Vcam1	-1.67	0.0000
Vezf1	1.72	0.0008
Vwf	2.48	0.0000
Myl4	2.34	0.0000
Mef2a	1.36	0.0022

Array 3

Gene	Fold	p-value
Agt	-3.78	0.0000
Agtr1a	1.27	0.5568
Agtr1b	2.50	0.0308
Agtr2	2.20	0.0416
Akt1	1.06	0.5027
Asf1a	1.45	0.0000
Atg5	1.30	0.0000
Atm	1.60	0.0003
Bax	1.47	0.0006
Bcl2	1.72	0.0000
Becn1	1.27	0.0000
Blm	2.57	0.0000
Pcgf4	1.89	0.0000
Brca1	2.83	0.0000
Bre	1.36	0.0004
Bub1b	2.39	0.0000
Cdkn1a	2.95	0.0000

Gene	Fold	p-value
Cdkn1c	-1.79	0.0296
Cdkn2a	-1.34	0.0047
Clspn	2.57	0.0000
Ctnnb1	1.18	0.0024
Dclre1c	1.82	0.0002
Dll4	2.33	0.0836
Esrrb	1.56	0.0110
Fen1	2.27	0.0001
Foxo3a	1.07	0.4284
Gadd45a	6.41	0.0000
Gsc	-1.07	0.6679
Gsk3b	1.49	0.0000
Hes1	2.71	0.0000
Hey1	2.08	0.0920
Hgf	-1.16	0.0301
Id2	1.23	0.0091
Igfbp3	1.60	0.0336

Gene	Fold	p-value
Igfbp4	2.43	0.0000
Igfbp5	-2.06	0.0001
Itih1	1.43	0.3661
Jag2	1.60	0.3764
Lif	15.56	0.0000
Lig4	1.30	0.4942
Maml1	2.06	0.0000
Mdc1	1.95	0.0000
Mdm2	2.03	0.0000
Met	-1.00	1.0000
Mitf	1.32	0.0072
Mixl1	3.12	0.0063
Mre11a	1.79	0.0006
Nanog	1.41	0.2240
Nbn	1.23	0.1566
Ogg1	1.06	0.4458
Parp1	1.45	0.0092

Gene	Fold	p-value
Pdgfa	-1.01	0.9123
Pdgfb	2.33	0.0151
Pim1	3.03	0.0000
Pot1	-1.79	0.0009
Rad17	1.65	0.0000
Rad50	1.79	0.0000
Rad51	2.99	0.0000
Ren1	2.53	0.0007
Sqstm1	1.60	0.0002
Sirt1	2.33	0.0000
Sirt6	1.09	0.0052
Smg5	2.99	0.0001
Est1a	1.97	0.0000
Smg7	2.99	0.0000
Smyd3	1.15	0.1236
Taf1	1.62	0.0000
Tbx3	1.36	0.0033

Gene	Fold	p-value
Tcl1	1.21	0.0178
Terf1	2.08	0.0000
Terf2	2.27	0.0000
Topbp1	2.23	0.0000
Upf2	1.95	0.0000
Upf3a	1.97	0.0000
Upf3b	2.64	0.0000
Wnt10b	1.10	0.2687
Wnt11	-1.00	1.0000
Wnt3a	1.09	0.7654
Xrcc4	1.34	0.0002
Xrcc5	-1.12	0.4033
Xrcc6	1.18	0.0078
Ercc2	1.95	0.0000
Hira	1.72	0.0018
Wrn	1.15	0.0610
Zfp42	2.33	0.0715

Supplemental Figure IV B

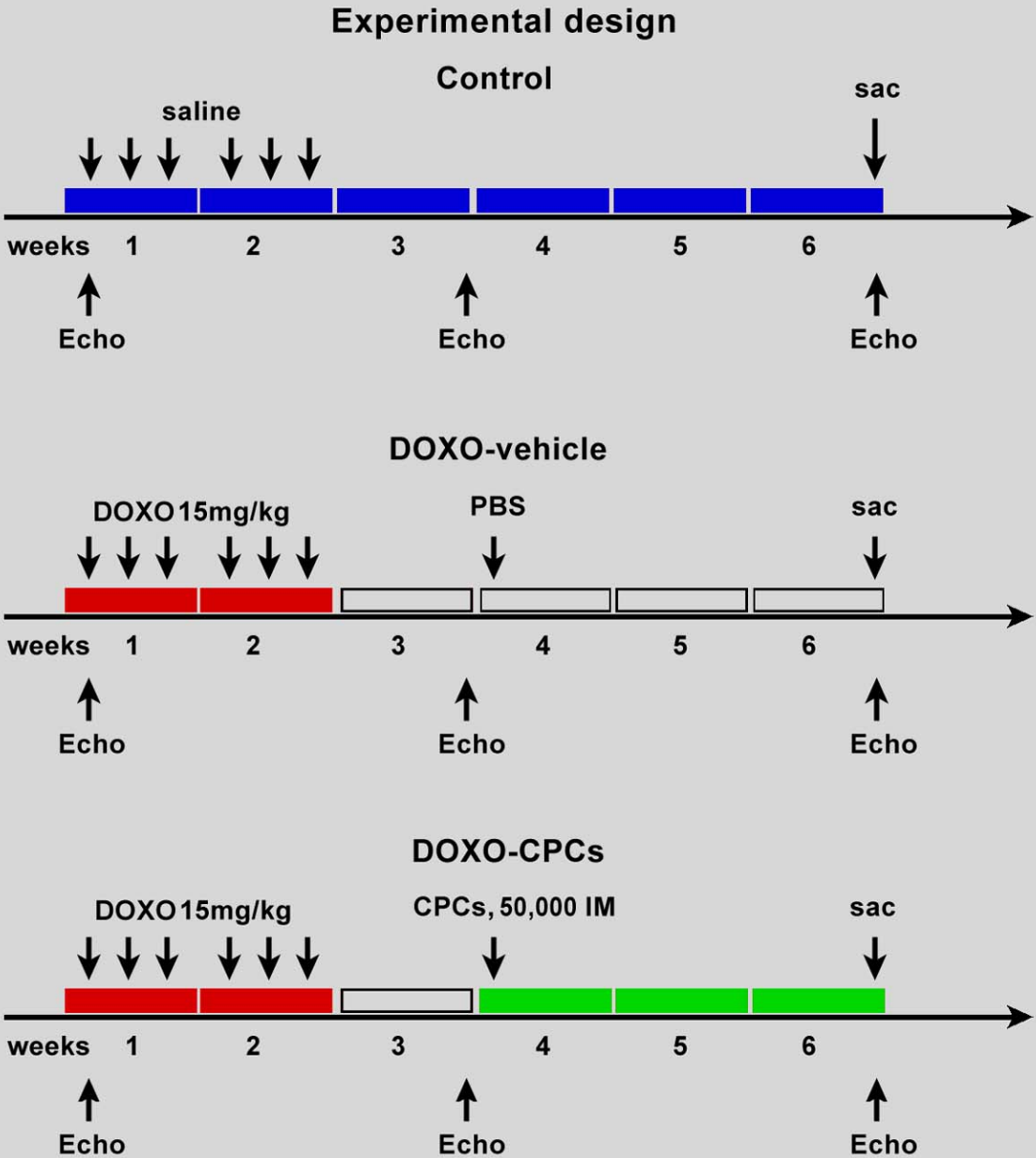

Supplemental Figure V

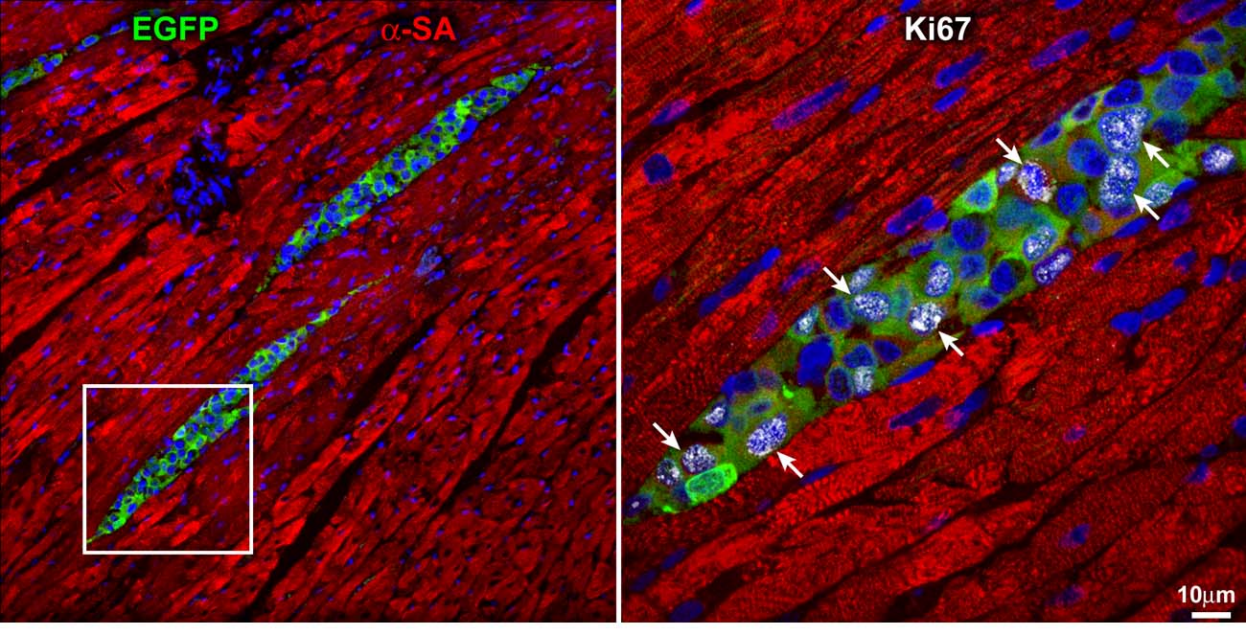

Supplemental Figure VI

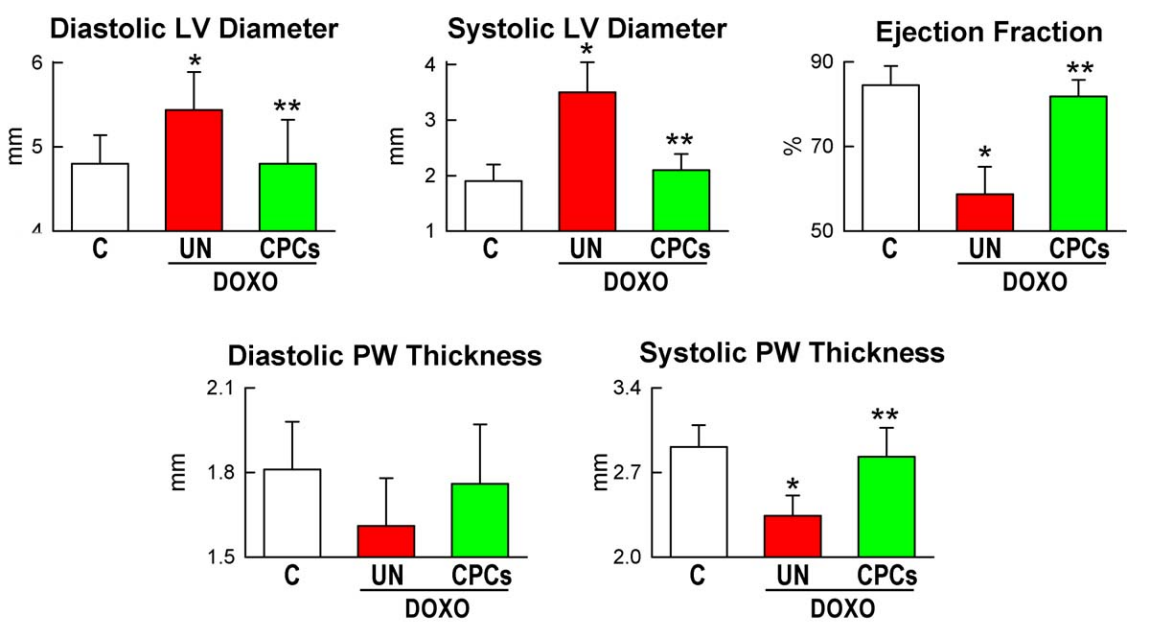

Supplemental Figure VII

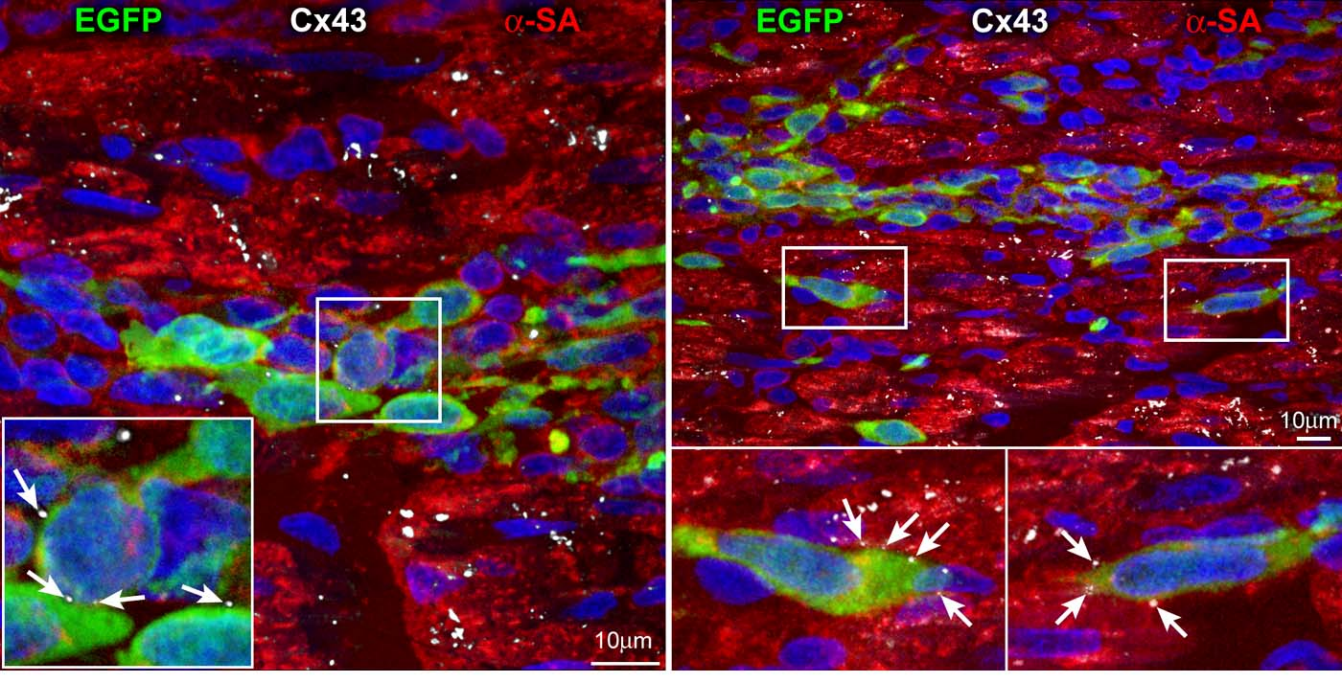

Supplemental Figure VIII

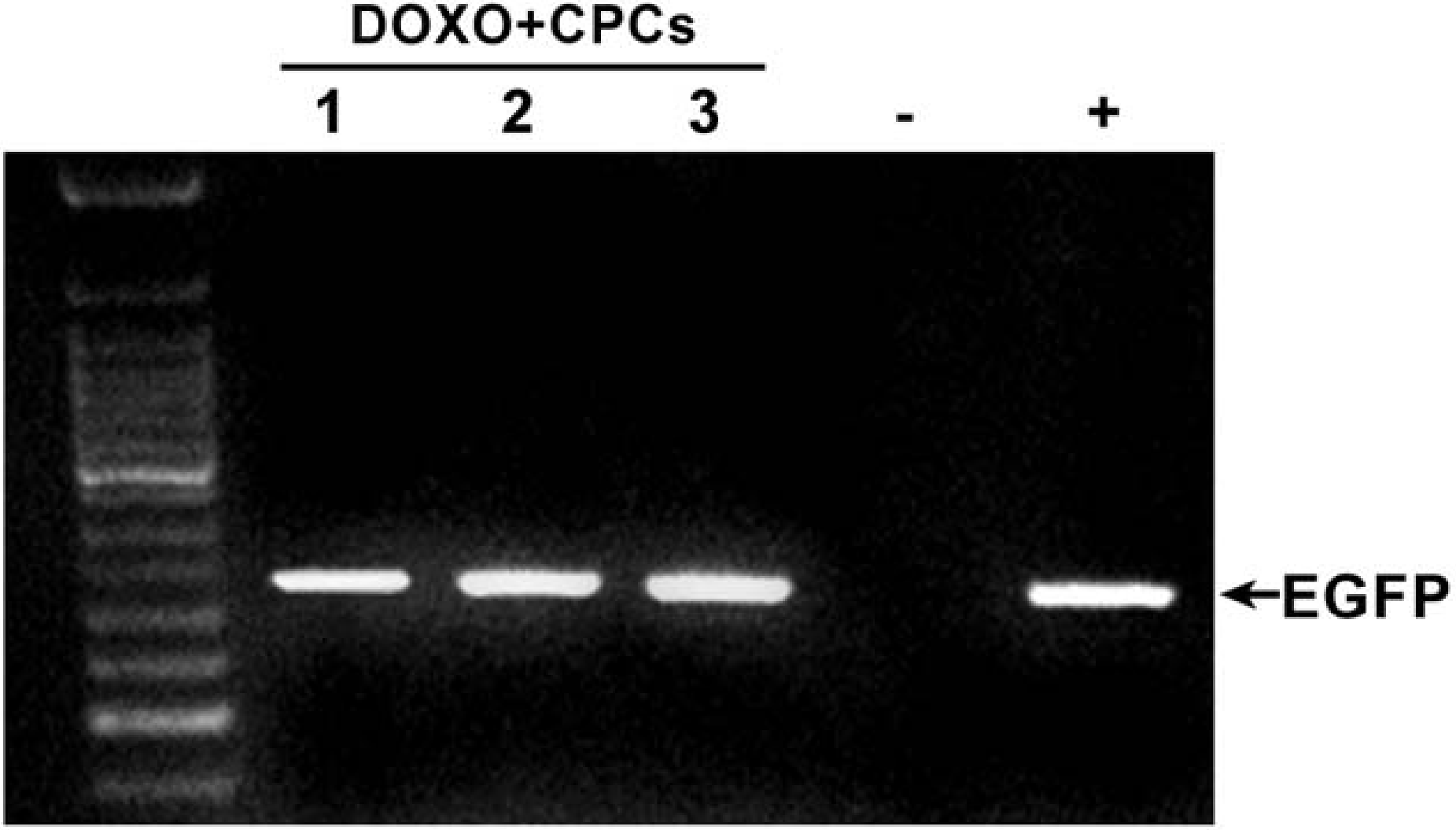

Supplemental Figure IX

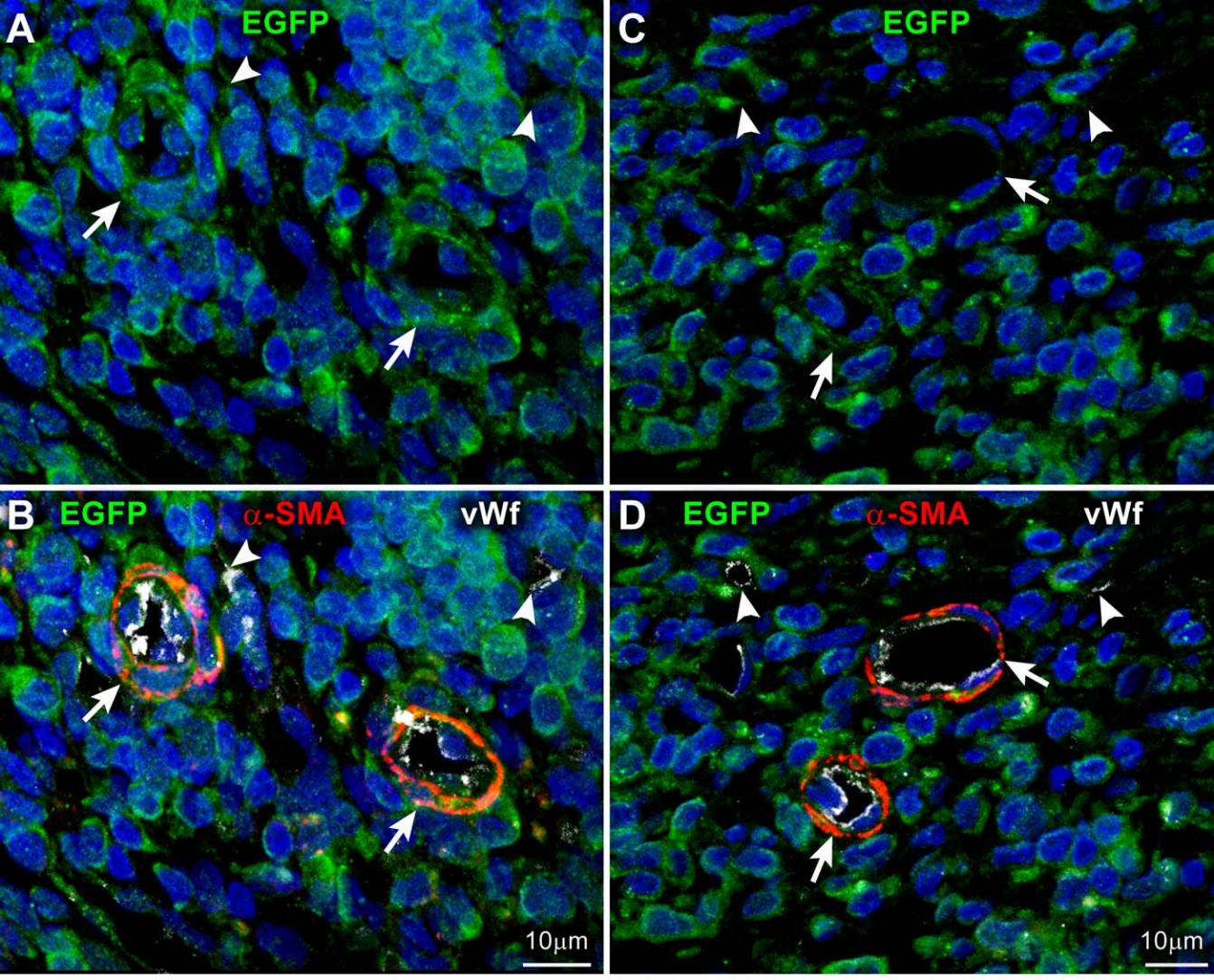

Supplemental Figure X

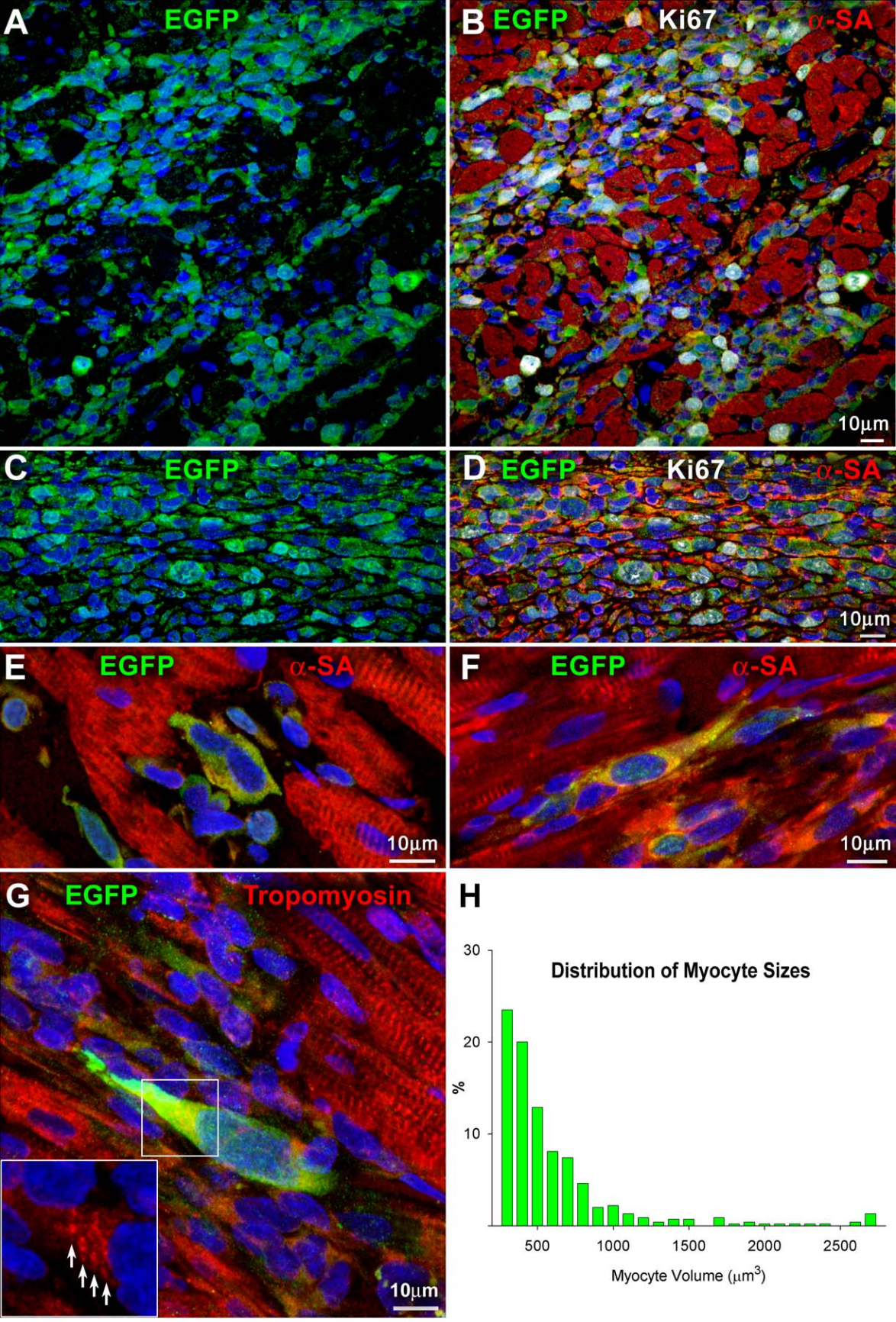

Supplemental Figure XI

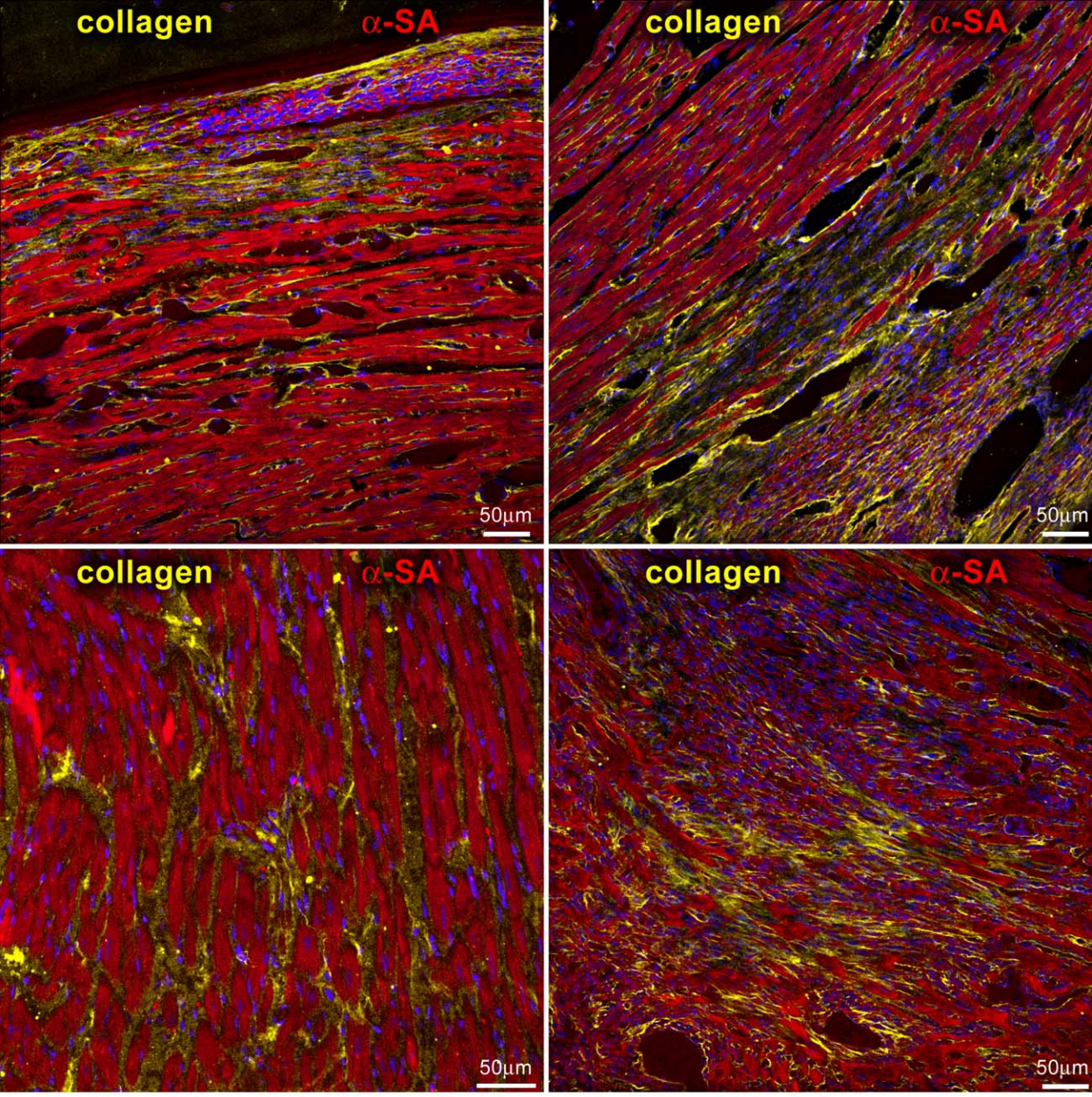

Supplemental Figure XII

Supplemental Figure Legends

Figure I. Cell cycle regulators. The expression of cyclins (**A**), cyclin-dependent kinases (**A**), retinoblastoma (**A**), and cell cycle inhibitors (**B**) was measured by Western blotting in CPCs in the absence and presence of DOXO.

Figure II. Oxidative stress and p53. (**A**) The expression of the antioxidant enzymes manganese superoxide dismutase (SOD), copper/zinc SOD and catalase was not affected by DOXO in CPCs. (**B**) ATM kinase and phosphorylated p53 at Ser 15 and 20 are upregulated in CPCs exposed to DOXO. Protein expression is shown as fold changes with respect to control (**C**).

Figure III. Experimental design. Time and doses of DOXO administration are shown schematically.

Figure IV. Transcriptional profile. **A and B**, Changes in gene expression in DOXO-treated CPCs are shown as fold differences with respect to control cells.

Figure V. Experimental design. Time, doses and modality of CPC administration are shown schematically.

Figure VI. CPC transplantation and DOXO-induced cardiomyopathy. Shortly after cell delivery, EGFP-positive (green) CPCs are organized in clusters within the myocardial interstitium. The area included in the square is shown at higher magnification in the adjacent panel. The majority of CPCs is cycling as documented by the expression of Ki67 (white). Myocytes are identified by α-SA (red).

Figure VII. Cardiac function. Echocardiographic measurements in control rats (C) and in rats treated with vehicle (UN) and cells (CPCs). *,**P <0.05 vs. C and UN, respectively.

Figure VIII. CPC engraftment. Connexin 43 (white, arrows) is expressed between CPCs (EGFP, green) and between CPCs and surrounding myocytes (α-SA, red). This cell-to-cell interaction is more apparent in the insets at higher magnification.

Figure IX. EGFP expression. DNA sequence of EGFP by PCR is evident in samples of regenerated myocardium from treated rats (DOXO+CPCs). Tail of β-actin-EGFP

transgenic mice was used as positive control (+) and myocardium obtained from untreated rats (-) was used as negative control.

Figure X. Vessel regeneration. Panels A and B, and panels C and D represent the same fields. The wall of newly formed small resistance arterioles (arrows) is composed of EGFP-positive smooth muscle cells (α-SMA, red) and endothelial cells (von Willebrand factor, white). EGFP-positive regenerated capillaries are also visible (arrowheads).

Figure XI. Myocardial regeneration. **A-D**, Large clusters of newly formed myocytes are identified by EGFP (A, C: green) and a-SA (B, D: red). Regenerated myocytes are small in size and are cycling (B, D: Ki67, white). **E-G**, More mature myocytes are present within the regenerated myocardium. At times, sarcomere striation is apparent (G, arrows). Cells express EGFP (green) and α-SA (red) or tropomyosin (red). **H**, Volume distribution of regenerated myocytes.

Figure XII. Replacement fibrosis. Foci of fibrosis are identified by collagen (yellow) accumulation.

Supplemental References

1. Beltrami AP, Barlucchi L, Torella D, Baker M, Limana F, Chimenti S, Kasahara H, Rota M, Musso E, Urbanek K, Leri A, Kajstura J, Nadal-Ginard B, Anversa P. Adult cardiac stem cells are multipotent and support myocardial regeneration. Cell. 2003; 114:763-776.
2. Gewirtz DA. A critical evaluation of the mechanisms of action proposed for the antitumor effects of the anthracycline antibiotics adriamycin and daunorubicin. Biochem. Pharmacol. 1999; **57**:727-741.
3. Linke A, Müller P, Nurzynska D, Casarsa C, Torella D, Nascimbene A, Castaldo C, Cascapera S, Böhm M, Quaini F, Urbanek K, Leri A, Hintze TH, Kajstura J, Anversa P. Stem cells in the dog heart are self-renewing, clonogenic, and multipotent and regenerate infarcted myocardium, improving cardiac function. Proc. Natl. Acad. Sci. USA. 2005; 102:8966-8971.

4. Rota M, LeCapitaine N, Hosoda T, Boni A, De Angelis A, Padin-Iruegas ME, Esposito G, Vitale S, Urbanek K, Casarsa C, Giorgio M, Lüscher TF, Pelicci PG, Anversa P, Leri A, Kajstura J. Diabetes promotes cardiac stem cell aging and heart failure, which are prevented by deletion of the p66shc gene. Circ. Res. 2006; 99:42-52.
5. Olivetti G, Abbi R, Quaini F, Kajstura J, Cheng W, Nitahara JA, Quaini E, Di Loreto C, Beltrami CA, Krajewski S, Reed JC, Anversa P. Apoptosis in the failing human heart. N. Engl. J. Med. 1997; 336:1131-1141.
6. Sun Y, Oberley LW, Li Y. A simple method for clinical assay of superoxide dismutase. Clin. Chem. 1988; 34:497-500.
7. Cohen G, Kim M, Ogwu V. A modified catalase assay suitable for a plate reader and for the analysis of brain cell cultures. J. Neurosci. Methods. 1996; 67:53-56.
8. Bearzi C, Rota M, Hosoda T, Tillmanns J, Nascimbene A, De Angelis A, Yasuzawa-Amano S, Trofimova I, Siggins RW, Lecapitaine N, Cascapera S, Beltrami AP, D'Alessandro DA, Zias E, Quaini F, Urbanek K, Michler RE, Bolli R, Kajstura J, Leri A, Anversa P. Human cardiac stem cells. Proc. Natl. Acad. Sci. USA. 2007; 104:14068-14073.
9. Urbanek K, Torella D, Sheikh F, De Angelis A, Nurzynska D, Silvestri F, Beltrami CA, Bussani R, Beltrami AP, Quaini F, Bolli R, Leri A, Kajstura J, Anversa P. Myocardial regeneration by activation of multipotent cardiac stem cells in ischemic heart failure. Proc. Natl. Acad. Sci. USA**.** 2005; 102:8692-8697.
10. Gonzalez A, Rota M, Nurzynska D, Misao Y, Tillmanns J, Ojaimi C, Padin-Iruegas ME, Müller P, Esposito G, Bearzi C, Vitale S, Dawn B, Sanganalmath SK, Baker M, Hintze TH, Bolli R, Urbanek K, Hosoda T, Anversa P, Kajstura J, Leri A. Activation of cardiac progenitor cells reverses the failing heart senescent phenotype and prolongs lifespan. Circ. Res. 2008; 102:597-606.

11. Siveski-Iliskovic N, Kaul N, Singal PK. Probucol promotes endogenous antioxidants and provides protection against adriamycin-induced cardiomyopathy in rats. Circulation. 1994; 89:2829-2835.
12. Kajstura J, Rota M, Whang B, Cascapera S, Hosoda T, Bearzi C, Nurzynska D, Kasahara H, Zias E, Bonafé M, Nadal-Ginard B, Torella D, Nascimbene A, Quaini F, Urbanek K, Leri A, Anversa P. Bone marrow cells differentiate in cardiac cell lineages after infarction independently of cell fusion. Circ. Res. 2005; 96:127-137.
13. Tillmanns J, Rota M, Hosoda T, Misao Y, Esposito G, Gonzalez A, Vitale S, Parolin C, Yasuzawa-Amano S, Muraski J, De Angelis A, Lecapitaine N, Siggins RW, Loredo M, Bearzi C, Bolli R, Urbanek K, Leri A, Kajstura J, Anversa P. Formation of large coronary arteries by cardiac progenitor cells. Proc. Natl. Acad. Sci. USA. 2008; 105:1668-1673.
14. Boni A, Urbanek K, Nascimbene A, Hosoda T, Zheng H, Delucchi F, Amano K, Gonzalez A, Vitale S, Ojaimi C, Rizzi R, Bolli R, Yutzey KE, Rota M, Kajstura J, Anversa P, Leri A. Notch1 regulates the fate of cardiac progenitor cells. Proc. Natl. Acad. Sci. USA**.** 2008; 105:15529-15534.
15. Anversa P, Olivetti G. Cellular basis of physiological and pathological myocardial growth. In: Page, E., Fozzard, H.A. & Solaro, R.J., eds. Handbook of Physiology. New York: Oxford Univ. Press. 2002; 75-144.
16. Urbanek K, Cesselli D, Rota M, Nascimbene A, De Angelis A, Hosoda T, Bearzi C, Boni A, Bolli R, Kajstura J, Anversa P, Leri A. Stem cell niches in the adult mouse heart. Proc. Natl. Acad. Sci. USA. 2006; 103:9226-9231.
17. Rota M, Hosoda T, De Angelis A, Arcarese ML, Esposito G, Rizzi R, Tillmanns J, Tugal D, Musso E, Rimoldi O, Bearzi C, Urbanek K, Anversa P, Leri A, Kajstura J. The young mouse heart is composed of myocytes heterogeneous in age and function. Circ. Res. 2007; 101:387-399.
18. Rota M, Padin-Iruegas ME, Misao Y, De Angelis A, Maestroni S, Ferreira-Martins J, Fiumana E, Rastaldo R, Arcarese ML, Mitchell TS, Boni A, Bolli R, Urbanek K,

Hosoda T, Anversa P, Leri A, Kajstura J. Local activation or implantation of cardiac progenitor cells rescues scarred infarcted myocardium improving cardiac function. Circ. Res. 2008; 103:107-116.